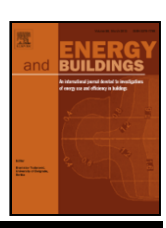
FISEVIER

Contents lists available at ScienceDirect

## **Energy & Buildings**

journal homepage: www.elsevier.com



# Experimental performance evaluation of a convective thermoelectric building envelope for building heating and cooling

Xiaoli Liu<sup>a, b, k</sup>, Kazuaki Yazawa<sup>c</sup>, Ming Qu<sup>a, b, \*</sup>, Orkan Kurtulus<sup>b</sup>, Brian Norton<sup>d</sup>, Niall Holmes<sup>e</sup>, Ruchita Jani<sup>e</sup>, Jorge Kohanoff<sup>f</sup>, Lorenzo Stella<sup>g, h</sup>, Conrad Johnston<sup>i</sup>, Hongxi Yin<sup>j</sup>

- <sup>a</sup> Lyles School of Civil Engineering, Purdue University, West Lafayette, IN 47906, USA
- <sup>b</sup> Ray W. Herrick Laboratories, Purdue University, West Lafayette, IN 47906, USA
- <sup>c</sup> Birck Nanotechnology Center, Purdue University, West Lafayette, IN 47906, USA
- <sup>d</sup> International Energy Research Centre, Tyndall National Institute, University College Cork, Cork, Ireland
- e School of Civil and Structural Engineering, Technological University Dublin, Dublin, Ireland
- f Instituto de Fusion Nuclear "Guillermo Velarde", Universidad Politecnica de Madrid, Madrid, Spain
- <sup>8</sup> Atomistic Simulation Centre, School of Mathematics and Physics, Queen's University Belfast, Belfast, United Kingdom
- <sup>h</sup> School of Chemistry and Chemical Engineering, Queen's University Belfast, Belfast, United Kingdom
- <sup>i</sup> Pacific Northwest National Laboratory, Richland, WA 99354, USA
- <sup>j</sup> Sam Fox School of Design and Visual Arts, Washington University in St Louis, St Louis, MO 63130, USA
- k Multifunctional Equipment Integration Group, Oak Ridge National Laboratory, Oak Ridge, TN 37830, USA

#### ARTICLE INFO

#### Article history: Received 30 April 2022 Received in revised form 15 July 2022 Accepted 9 August 2022

Keywords:
Thermoelectric building envelope
Heating and cooling
Prototype evaluation
Experiment

#### ABSTRACT

The thermoelectric building envelope (TBE) integrates thermoelectric materials with the building envelope for active space heating and cooling. The advantage of TBE heating and cooling includes its significantly low-profile design and no refrigerant use. Although there are existing studies evaluating TBE performance, they were based on limited operating conditions. The study aims to experimentally evaluate the heating and cooling performance of a TBE prototype under various operating conditions. The TBE prototype was installed between two psychrometric chambers, which simulated indoor and outdoor conditions. The prototype was tested at an indoor temperature of around 22.35–23.58 °C and outdoor temperatures from –7.35 °C and 16.99 °C for heating and from 28.36 °C to 40.95 °C for cooling, with varied power inputs and fan conditions. The maximum coefficient of performance (COP) of TBE in heating mode is 3.2. The average heating COP of TBE with a current of 1.5 A in four winter scenarios is 1.37. The average heating COP of TBE operating with the current of 0.3–1.5 A at an outdoor temperature of 12 °C is 2.27. The TBE system demonstrates a better heating efficiency than an auxiliary electric heater for the heat pump system. The experimental results and evaluation obtained provide critical guidance for the deployment of TBE applications.

© 20XX

#### Nomenclature Abbreviation Description AC Alternative current COP Coefficient of performance DC Direct current Thermoelectric building envelope TBE Thermoelectric module TEM Description (Unit) Symbol Area $(m^2)$ A $c_p$ Heat capacity at constant pressure $(J/kg \bullet K)$ Heat per second (W)

 R Electrical resistance  $(\Omega)$ 
 $R_{th}$  Thermal resistance (K/W) 

 S
 Seebeck coefficient (V/K) 

 T Temperature  $(^{\circ}C)$  

 V Voltage (V) 

 I Current (A) 

 P Power (W) 

 K Thermal conductance (W/K) 

  $\sigma$  Electrical conductivity (S/m) 

https://doi.org/10.1016/j.enbuild.2022.112376

0378-7788/© 20XX

#### 1. Introduction

Buildings in the United States are responsible for 40% of the country's total energy use and 39% of total greenhouse gas emissions [1]. As society continues to deal with the ongoing energy crisis and environmental deterioration, researchers seek new technologies to reduce building energy consumption and greenhouse gas emissions. Thermoelectric technology is one such technology as it can convert differences in temperature to electrical energy or reversely. This conversion from thermal to electrical energy using thermoelectric materials resulting in a power generation is called the Seebeck effect, whereas the conversion of electrical to thermal energy leading to temperature regulation is called the Peltier effect [2].

Researchers have investigated thermoelectric technology applied to buildings [3-5]. One promising application is to integrate thermoelectric materials in the building envelope for power generation and space heating and cooling without the requirements of transporting energy and synergy among subsystems. As shown in Fig. 1, in summer, the thermoelectric building envelope (TBE) can cool the indoor space and maintain thermal comfort by absorbing heat via radiation and convection. The TBE can heat the indoor space in winter, given an opposite current input. The operation of the TBE possesses many merits. Firstly, the TBE system can operate with renewable energy such as directcurrent (DC) power from photovoltaic panels. This system saves fossil fuels and eliminates the electricity loss from DC/AC conversion. Hence, it is one of the enablers for net-zero energy and CO2 emission buildings [3,6-8]. Secondly, the TBE system eliminates refrigerant use and hydrofluorocarbon emissions from conventional air conditioning systems. Hydrofluorocarbon, one of the greenhouse gases, decreases the ozone layer in our atmosphere, making the earth more vulnerable to climate change [9]. Additionally, the compact design of TBE allows reducing the energy loss due to transportation among subsystems. Finally, the thermoelectric system can provide reliable operation with a low maintenance cost, accurate temperature regulation, and rapid response [10].

The study of TBE is still at an early stage. A mathematical model proposed by Khire et al. in 2005 [11], indicated that a TBE design with 340 thermoelectric couples could meet a cooling load of 6 W for an enclosed space. Theoretically, the system's COP, considering fan power, can reach 1.5 when the temperature difference between outdoor and indoor air is 18 °C. A decade later, experimental investigations on the TBE system were carried out [11-18]. In 2015, Liu et al. tested the performance of a thermoelectric radiant wall powered by PV panels. Ten commercially available thermoelectric modules (TEMs) were attached to an aluminum panel for indoor radiant heating [13] and cooling [12]. Test results showed that the system decreased the surface temperature of a radiant panel to 3-8 °C lower than the indoor air temperature, with a cooling density of 42 W per unit m<sup>2</sup> panel in summer. The same system increased the panel surface temperature to about 29 °C higher than the indoor air temperature, with a heating capacity of 36 W/m<sup>2</sup> in winter. A heating COP of 2.3 was reported, primarily due to the contribution of a smaller temperature difference between indoor and outdoor air (<4 °C), a lower surface temperature of radiant panels (<34 °C), and reduced power consumption of the ventilation fan. Another TBE system with three TEMs was developed and tested by Wang et al. to heat a onem<sup>3</sup> adiabatic box at an outdoor air temperature of 2-4 °C, demonstrating a COP of around 1.8-3.9 excluding fan power consumption [14]. The heat sink has a base area 7.6 times larger than the TEMs, which benefited the overall system performance. This study also reported that an energy-saving of 64% and a reduction of CO2 emission of 4305 kg/ year could be possible by utilizing solar and wind energy [14]. Meanwhile, four real-scale ventilated active TBEs were studied by a research

E-mail address: mqu@purdue.edu (M. Qu).

group in Spain with a focus on architects and constructions [15-19]. The first three prototypes demonstrated the possibility of TBE for space heating and cooling and the efforts to create modular TBE devices for integrating energy systems in architectures. The fourth prototype aimed to improve the heat deliverable and COP by considering four key design parameters: the number of cells, control system, insulation, and components such as heatsinks and fans. A cooling COP of 0.64–0.94 and a cooling capacity of 76–133 W for sixteen TEMs were obtained with the outdoor temperature varying between 26 and 33 °C and a heating COP of 0.82–1.01 and a heating capacity of 82–155 W for sixteen TEMs were obtained with the indoor temperature varying between 6 and 13 °C. The forced convection enhances the heat transfer at the boundary and favors the thermal capacity of TEMs but as a result lowers the overall COP with fan power.

It is found from the literature that the performance of TBE is not only a function of surface temperature differences determined primarily by the power input and heat dissipation rate but also related to the temperature difference between indoor and outdoor air. However, limited experimental investigations were conducted to evaluate the heat pumping performance of TBE to study the impact of varying operating conditions, especially the outdoor air temperature. Hence, many research gaps and challenges still exist to the effective use and application of TBE systems.

First, most studies in the literature tested the TBE under outdoor conditions, which are limited and uncontrollable due to the variation of ambient conditions. In the heating scenario, the outdoor temperature was higher than 5 °C in the heating scenario, a very mild condition in winter. However, the outdoor condition influences the TBE performance significantly. Assessment of the TBE performance reported cannot represent the system performance under different outdoor conditions or climate zones. Therefore, TBE evaluation under various controllable outdoor conditions is highly needed to evaluate TBE's performance and provide experimental data for further studies, including model validation.

Second, the COP calculation of a TBE system in the literature remains insufficient consideration, including assumptions' validity and system-level analysis. Many tests [15-18] examined the TBE under the unsteady outdoor air temperature fluctuating in the range of 5 to 10 °C. It leads to higher uncertainty and errors in TBE behavior evaluation as the performance indicators calculated from the analytical model are based on assumptions valid in steady-state conditions. With the change in outdoor temperatures, the heat flux calculation through a building envelope with non-ignorable thermal mass will not be accurate as a dynamic proportion of energy is absorbed into the envelope. Wang et al. [14], for instance, presented the system COP 10 min after test start-up. This COP calculation reflected the prototype's performance at transient states, where the energy balance and flow are significantly different from a steady state. Second, the simplified model used in the literature is not suitable for COP calculation of a transient thermal system, as the ignorance of heat storage in thermal mass concerning time is not valid for a transient system.

Besides, Liu *et al.* [13] found that the surface temperature difference that commercial TEM can hold was within 5–25 °C, primarily due to the Peltier effect and the nature of heat conduction. This indicates that the TEM may not be effective and efficient if the surface temperature exceeds 25 °C, since a larger amount of heat flux is lost by conduction. However, in a cold climate, the air temperature difference between indoor and outdoor air may already exceed 25 °C. Therefore, it is essential to design and develop a TBE system with optimized TEM designs for different climate zones.

This work addresses the three primary research gaps and challenges in designing, assembling, and testing a TBE prototype. The TBE prototype in this work was developed by using three commercially available TEMs connected both thermally and electrically in series and then evaluated between two psychrometric chambers with controllable air con-

Corresponding author at: Civil Engineering Building, 550 Stadium Mall Drive, West Lafayette, IN 47907-2051.

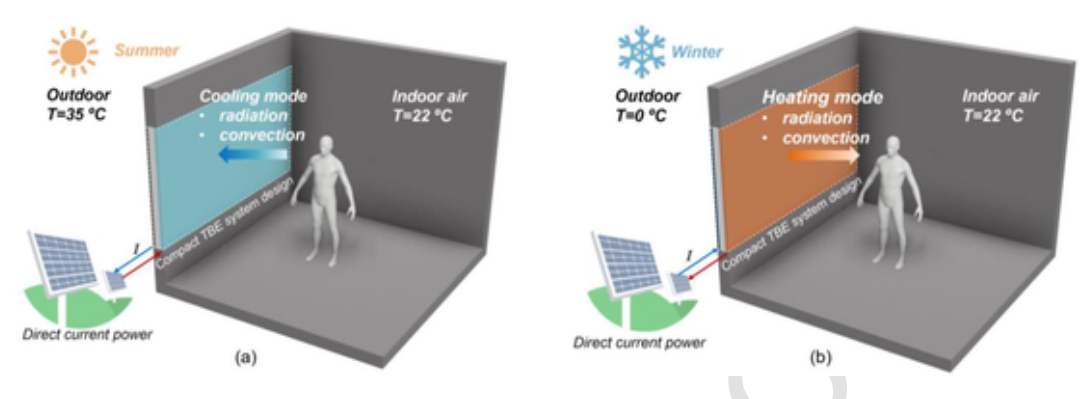


Fig. 1. Conceptual diagrams of use scenarios of TBE: (a) cooling mode in summer and (b) heating mode in winter.

ditions. The tested outdoor air temperatures were controlled under a wide range of different steady-state conditions (-7.35–16.99 °C in heating and 28.36–40.95 °C in cooling). An analytical model developed provides performance analysis of the TBE prototype, including thermal capacity, effective thermal capacity, and COP. This paper is organized as follows: A methodology overview is given in *Section 2*, a detailed description of the experimental methods is given in *Section 3*, and a description of the analytical modeling methods is given in *Section 4*. Next, the test results, analysis, and discussions are presented in *Section 5*. Finally, *Section 6* concludes with the findings of this study.

## 2. Methodology overview

The study aims to design and construct a TBE and determine its performance in a laboratory environment. As illustrated in Fig. 2, the study includes four parts: Prototype design and assembly, test apparatus development, test procedure, and program, and result analysis.

For the design and construction of the TBE prototype (in Section 3.1), the commercially available TEMs were used and integrated with the building envelope, which consists of the rigid Expanded Polystyrene (XPS) insulation board as material and plywood panels for structural support. Heat sinks and DC-powered fans were adopted to transfer heat from TEMs to surroundings effectively.

For the test apparatus development (in *Section 3.2*), the TBE prototype was installed between two psychrometric chambers, which simulate indoor and outdoor conditions. Twelve thermocouples measured the indoor and outdoor temperatures, surface temperatures of the envelope and TEMs, and air temperature close to TBE. A power supply unit (PSU) provided the DC power to the TBE prototype.

For experimental conditions (in *Section 3.3*), variations in outdoor temperatures, power inputs, and fan conditions were considered. Three different outdoor temperatures were used for cooling. Four different outdoor temperatures were used for heating. The current flow from 0.3 A to 1.5 A was controlled and powered to the prototype. The impact of fan status on system performance was studied.

For performance indicator calculation (in *Section 4*), a widely used analytical model was employed. Combined with material properties obtained from the datasheet, the measured temperatures, and the operating conditions, the analytical model calculated the heat flux from the TBE prototype, the effective thermal capacity, and COP for heating and cooling (in *Section 5*).

#### 3. Experimental study

This section describes the methodological details of all the experimental work, including prototype design, construction, test setup, and testing procedures.

## 3.1. Prototype design and assembly

Fig. 3 is the schematic diagram of the TBE prototype. With a dimension of  $0.38 \times 0.38 \times 0.13$  m<sup>3</sup>, the prototype has three major parts: (1) the building composite wall, (2) the TEMs, and (3) the combination of heatsinks and fans. The building composite wall consists of a 12.7-mm (half-inch) thick rigid XPS board sandwiched between two 5-mm plywood boards. The TEMs include three high-performance commercially available TEMs, purchased from TE Technology, Inc. One TEM 127 (HP-127-1.4-2.5, with 127-pair thermocouples) was placed in the center with two TEMs 199 (HP-199-1.4-0.8, with 199-pair thermocouples) on either side. As shown in Fig. 3(c and d), they were connected thermally and electrically in series. This configuration enables the TBE to deliver adequate temperature differences for stable and effective space cooling and heating. The combination of two heat sinks with a height of 50 mm and a 12 V DC-powered fan was used to dissipate the heat to the surroundings. Thermal sheets and grease were applied to all interfaces among TEMs to reduce contact resistance. Table 1 includes the specifications of TEMs, heatsinks, and fans.

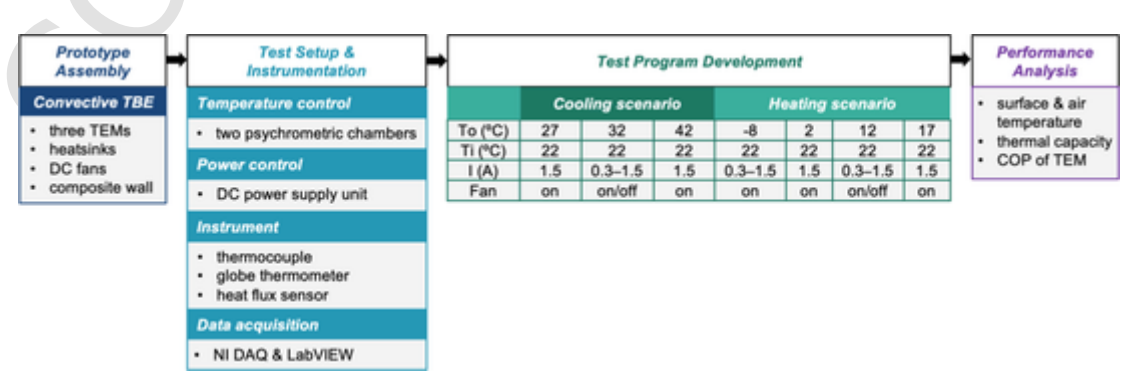


Fig. 2. An overview of the research methodology.

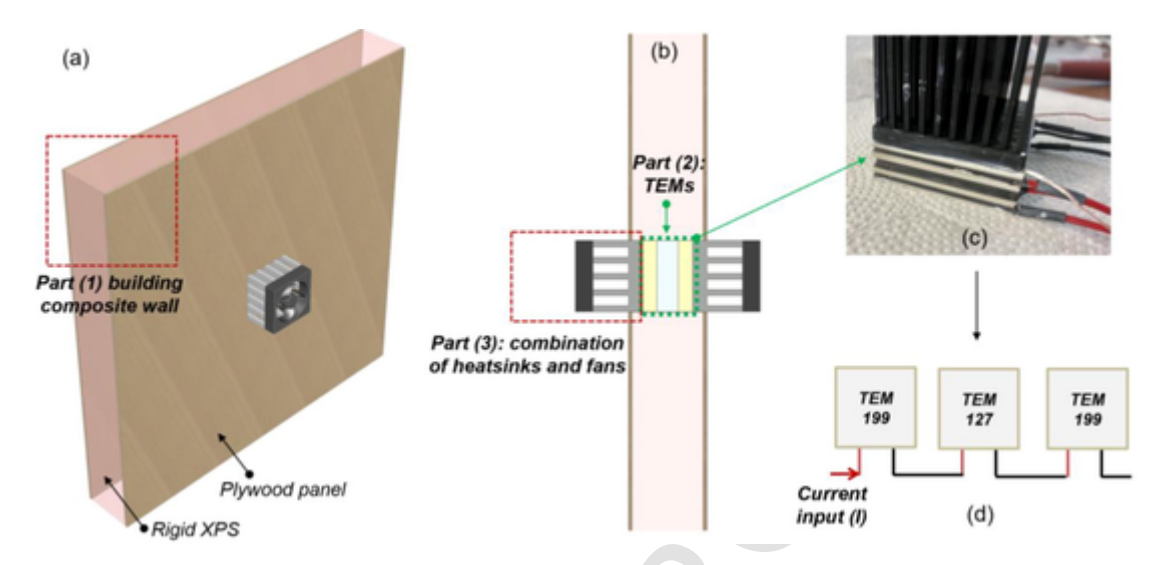


Fig. 3. (a) A 3D rendering image and (b) a cross-sectional view of a TBE prototype, (c) a photographic view of the TEM combination, and (d) a diagram of the electrical connection of TEMs.

**Table 1**Specifications of the TEMs, heatsinks, and fans.

Device	Model No.	Operation range	Size [mm × mm × mm]
TEM 199	HP-199-1.4-0.8	I<11.3A, V<24.6V -40°C <t<80°c< td=""><td>module: <math>40 \times 40 \times 3.2</math> element: <math>1.4 \times 1.4 \times 0.8</math></td></t<80°c<>	module: $40 \times 40 \times 3.2$ element: $1.4 \times 1.4 \times 0.8$
TEM 127	HP-127-1.4-2.5	I < 3.7A, V < 16.3V -40°C < T < 80°C	module: $40 \times 40 \times 4.9$ element: $1.4 \times 1.4 \times 2.5$
Heatsink	CS40-50B	Thermal R≈0.84K/W	$40\times40\times50$
Fan	F-4010H12BII- 12	V=7-12V, I=0.18A (rated) P=0.7W (calculated)	40×40×10

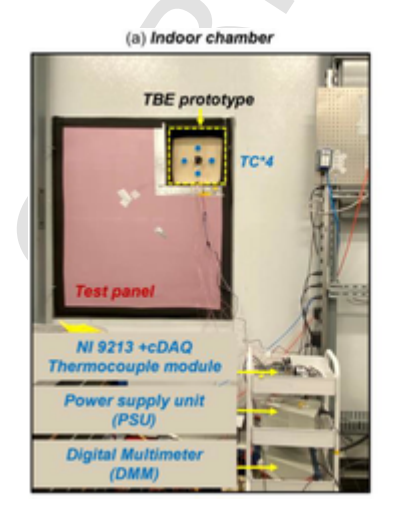
#### 3.2. Test apparatus

A test apparatus was built in the Herrick Labs at Purdue University to evaluate the TBE prototype. The apparatus comprised four parts: (1) the TBE prototype, (2) testing chambers, (3) sensors, and (4) the data acquisition system. As shown in Fig. 4, the developed TBE prototype was mounted in a test panel located on the interior wall between two chambers. A DC PSU was used to power the TEMs. Twelve thermocouples were used in the TBE prototype to measure temperatures of the interfaces between TEM and heatsinks, the interfaces between plywood

and XPS boards, the air near the indoor heat sink in four different directions, and the air far away (0.3 m) from the testbed. All thermocouples were connected to a National Instruments (NI) acquisition platform, which includes a 9213 module and a cDAQ device for data acquisition. A sample rate of 1 Hz was set for all channels and devices. Table 2 lists the specifications of the measurement instrumentation.

## 3.3. Test procedure

Seven tests as listed in Table 3 were conducted to evaluate the TBE prototype's performance under different operating conditions. The chamber for simulating the indoor conditions was set at a constant temperature, around 22.35–23.58 °C ( $T_{SA,in}$ ). Meanwhile, the other chamber simulating the outdoor conditions was set at different temperatures of 28.36, 32.17, and 40.95 °C for summer and –7.35, 2.20, 13.04, and 16.99 °C for winter. Current input varied from 0.3 to 1.5A and was controlled to avoid exceeding a surface temperature of 60 °C for safety operation. The fan status presents the operation of DC fans when the TBE prototype is powered. After psychrometric chambers reached the setpoints and at steady states, current inputs were applied to the TEMs for the system to achieve steady-state operations.



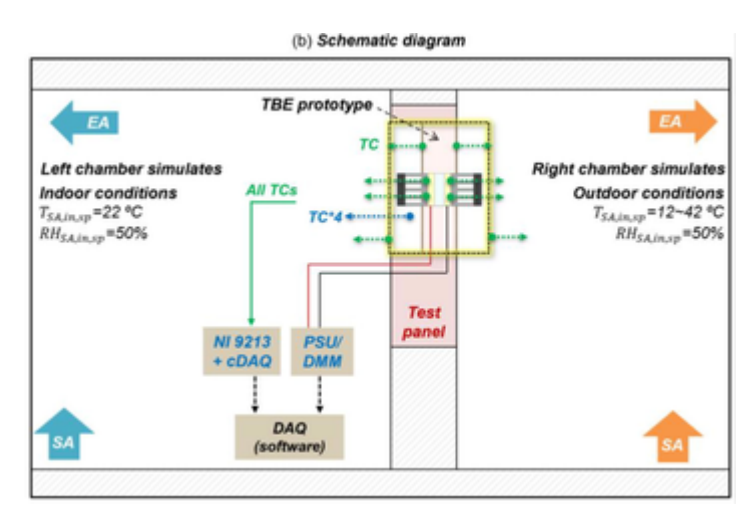


Fig. 4. (a) A photo of the testbed showing sensors and data acquisition system and (b) a schematic diagram of the test setup for evaluating TBE in psychrometric chambers.

 Table 2

 Specifications of the measurement instrumentation.

1				
Measured variable	Instrument	Operation range	Resolution	Uncertainty
TEM surface temperature	36 AWG K-type thermocouples	−270− 1260 °C	~41 µV/°C	±1.1 °C
Air temperature	30 A.W.G. T-type thermocouples	−270− 370 °C	~43 µV/°C	±0.5 °C
Current input	Siglent SPD1168X power supply unit	0–8 A	1 mA	±(0.3%× reading+ 10 mA)
Voltage input		0–16 V	1 mV	± (0.03% × reading + 10 mV)
TC input module	NI 9213 16-channel TC input module	V: ±78 mV T: -40- 70 °C	<0.02 °C 24 bits, 75 S/s	-
Data acquisition module	NI 9178 cDAQ	T: -20- 55 °C, RH : 10-90%	32 bits	-

**Table 3**Operating conditions for seven testing scenarios.

Test No.	Scenario	T <sub>SA,out</sub>	T <sub>SA,in</sub> [°C]	ΔT[°C]	RH [%]	I <sub>input</sub> [A]	Fan
1	Hot (day) cooling	40.95	22.91	18.60	50	1.5	On
2	Warm (day) cooling	32.17	22.92	9.25	50	0.3– 1.5	On
						0.7	Off
3	Cold (day) cooling	28.36	22.35	5.45	50	1.5	On
4	Hot (day) heating	16.99	22.77	-5.78	50	1.5	On
5	Warm (day) heating	13.04	22.61	-9.57	50	0.3– 1.5	On
						0.7	Off
6	Cold (day) heating	2.20	23.58	-21.38	50	1.5	On
7	Coldest (day) heating	-7.35	23.34	-30.69	50	1.5	On

## 4. Analytical model and performance indicator

#### 4.1. Performance indicator

The indicators selected for performance evaluation include measured parameters: Hot-side surface temperature ( $T_h$  [°C]), cold-side surface temperature ( $T_c$  [°C]), and the air temperature close to the TEMs, and derived indicators: Heating capacity ( $\dot{Q}_h$  [W]), cooling capacity ( $\dot{Q}_c$  [W]), COP ( $COP_h$  and  $COP_c$ ), and COP including fan power ( $COP_{h,fan}$  and  $COP_{c,fan}$ ).

## 4.2. Analytical thermoelectric model

A well-known analytical model based on energy conversion and thermoelectric principles was used to calculate the performance of thermoelectric materials according to material properties and operating conditions [2]. TEM can pump heat from one end to the other with a suitable power input in the heat pump mode due to heat absorption and dissipation at the boundary when electric charge carriers move between dissimilar materials with various electrochemical potentials. The main contribution to the heat transfer inside a thermoelectric material includes the Seebeck-Peltier effect, Fourier's law of conduction, and Joule heating. In this analytical model, the material's thermoelectric properties are assumed to be isotropic and independent of temperature. Thus, the Thomson heating, due to the temperature dependence of the Seebeck coefficient, gives a relatively smaller contribution, and it is ignored. Since the model is a steady-state model, the temperature changing with time, such as the heat storage in thermal mass, is also neglected when the temperature profiles are converged. Moreover, since the insulation material (XPS) has a low thermal conductivity of

0.029 W/mK, heat transfer from the TEMs to XPS is negligible. To model a TBE prototype, where three TEMs are stacked together, the heat transport equations of the i-th surface of TEM are written in Eq. (1) and Eq. (2) [20].

$$\dot{Q}_{hi} = S_i I T_{hi} - K_i \left( T_{hi} - T_{ci} \right) + 0.5 I^2 R_i \tag{1}$$

$$\dot{Q}_{ci} = S_i I T_{ci} - K_i \left( T_{bi} - T_{ci} \right) - 0.5 I^2 R_i \tag{2}$$

where S is the Seebeck coefficient; K is the thermal resistance, calculated by kA/L; and R is the electrical resistance, calculated by  $L/\sigma A$ . The properties of TEMs are provided by the manufacturer. The thermoelectric element in the TEM has a Seebeck coefficient (S) of about 208  $\mu$ V/K, thermal conductivity (k) equal to 1.6 W/(m²K), cross-sectional area (A) of 1.4×1.4 mm², a full leg length (L) of 2.5 mm for TEM 127 and 0.8 mm for TEM 199, and electrical conductivity  $\sigma$  by about 0.97×10<sup>5</sup> S/m.

The heat deliverable from TBE is considered the cooling power  $(\dot{Q}=\dot{Q}_c=\dot{Q}_{cl})$  during the cooling season, whereas that is considered as the heating power  $(\dot{Q}=\dot{Q}_h=\dot{Q}_{h3})$  in the heating season. Since the combination of TEMs is symmetric, both the top and bottom TEM's can operate as hot or cold ends. Meanwhile, because three TEMs are connected thermally in series, they share the same temperature and heat flux on the interfaces. Then heat deliverables can be computed by assigning boundary conditions to both cold and hot surfaces and solving the linear system.

The effective heat flux considers the heat transfer from the outdoor air to the indoor air through the insulation and plywood boards. Hence, the effective heating/cooling capacity of a TBE prototype can be expressed as Eq. (3).

$$\dot{Q}_{eff} = \dot{Q} - \dot{Q}_{wall} = \dot{Q} - \left(T_{xps,h} - T_{xps,c}\right) / R_{xps} \tag{3}$$

In addition, the heat flux density ( $\dot{q}_{TBE}$ , W/m²) is also a performance indicator to determine the number, the design, and the cost of TEMs. The heat flux density of the TBE prototype is expressed as Eq. (4), defined as the ratio of heating/cooling capacity to the cross-sectional surface area. The effective thermal capacity must be used for the calculation of heat flux density to account for the overall heat transfer from all parts of the TBE prototype.

$$\dot{q}_{TBE} = \dot{Q}_{eff}/A \tag{4}$$

The work applied to the system equals the difference in thermal capacity between the hot side and the cold side, primarily used for Peltier heat and against the electrical resistance, expressed as Eq. (5). The COP is the ratio of desired output to work required, as depicted in Eq. (6). without considering the external power consumption. The desired heat (Q) is the heating capacity  $(Q_h)$  in winter conditions, while it is the cooling capacity  $(Q_c)$  in summer conditions. TBE performance is also affected by fan power consumption. As a result, the COP considering fan power  $(COP_{fan})$  can be written in Eq. (7). The actual air velocity through the heat sink is obtained by finding the intersection of the pressure-velocity curve of the DC fan and the heat sink. The air velocity could also be checked by the thermal resistance-velocity curve of the heatsinks. After that, the fan power  $(W_{fan})$  can be obtained by the given air velocity.

$$P = \dot{Q}_h - \dot{Q}_c \tag{5}$$

$$COP = \dot{Q}/P \tag{6}$$

$$COP_{fan} = \dot{Q}/\left(P + W_{fan}\right) \tag{7}$$

The thermal capacity and COP analysis are carried out using uncertainty propagation, where neglecting correlations or assuming independent variables yields a typical variance formula [21]. As a result, the maximum thermal capacity and COP uncertainties are around  $\pm$  2.67 W and  $\pm$  0.10, respectively.

## 5. Result analysis and discussion

This section presents the heat pumping performance of the TBE prototype operating in both cooling and heating scenarios. The studied performances include the temperatures achieved by the TBE prototype, heating/cooling capacity, effective capacity, and COP. Using this data, the relationships between the predicted performance from the model and the primary operating parameters are analyzed by the experimental data obtained from sensitivity studies related to those parameters: Outdoor temperatures, current inputs, and fans.

#### 5.1. Heat pumping performances under various outdoor conditions

Fig. 5 shows the surface temperatures of the TBE prototype and air temperatures given a current input of 1.5 A under various outdoor conditions. The outdoor temperatures were 32.17 °C and 13.04 °C in the cooling and the heating season, respectively. The indoor temperature was at 23 °C. The two chambers first maintained constant indoor ( $T_{air,in}$ ) and outdoor air temperatures ( $T_{air,out}$ ). After the power was applied to the TBE prototype, the TBE prototype responded immediately with a significant temperature differential of around 43 °C (summer case) and 40.4 °C (winter case) between the indoor TEM surface,  $T_{TE,in}$  and outdoor TEM surface,  $T_{TE,out}$ . During the cooling test (Fig. 5(a)), the indoor surface decreased to 18 °C to provide cooling to the indoor space. In the heating mode (Fig. 5(b)), the indoor surface increased to 49 °C for heating the room air. Due to the forced convection introduced by DC fans, surface temperatures quickly reached a steady state. Once

the DC power input was removed, the surface temperature converged with that of the indoor and outdoor air.

As described in *Section 3.2*, four thermocouples were placed in four different orientations near the indoor heat sink to measure air temperatures close to the heat sink. As shown by the green shaded area in Fig. 5 (a), during the cooling season, the TBE reduced the nearby air temperature by approximately 3 °C. On the other hand, during the heating season, TBE raised the nearby air temperature by about 11 °C, as shown by the purple shaded area in Fig. 5(b). The comparison reveals that TBE has better performance for heating in winter than cooling in summer. In this heating test, the temperature lift of air was about 23 °C.

The surface temperatures of the insulations on both sides in the TBE prototype, which is the rigid XPS board, were recorded ( $T_{xps,in}$  and  $T_{xps,out}$  in Fig. 5). As may be seen, there is an increase in the temperature difference between the two sides of the insulation. Due to the increase in temperature difference, more heat fluxes through the XPS insulation board can cause a greater heat loss. The actual heating/cooling provided to the room needs to consider the increased heat loss. In the analytical calculation, the effective capacity of heating/cooling is defined by using the measured surface temperatures of XPS as an input.

Fig. 6 shows the performance of TBE operating in the three-repeated heating operation under an outdoor temperature of -7.35 °C. As can be seen, the TBE provided heating with a temperature increase of approximately 30 °C. The nearby air was heated to 33.4 °C at this outdoor temperature. Additionally, the operation of TBE is reliable in the three heating cycles within 1 °C of temperature changes. Surface

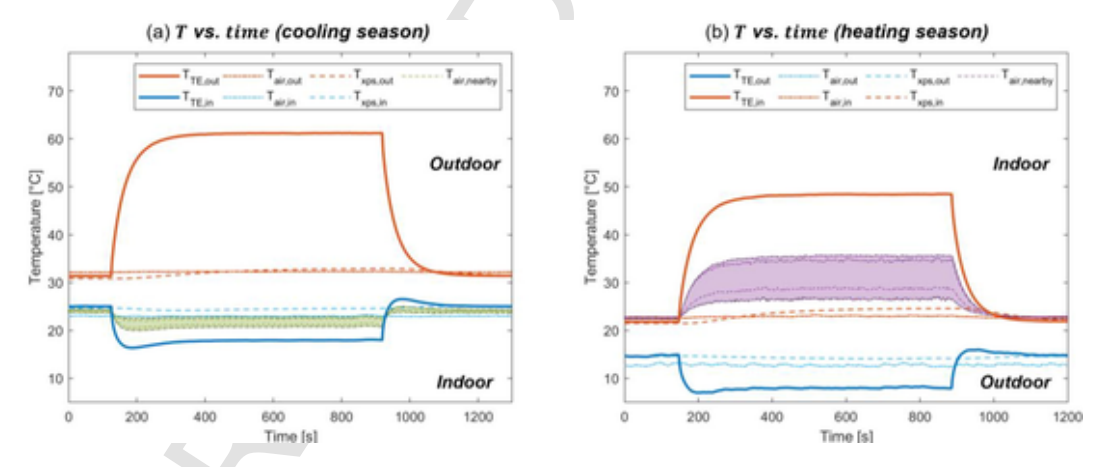


Fig. 5. Experimental temperature-time response of TBE in (a) the warm cooling scenario under  $T_{outdoor} = 32.17$  °C and (b) the warm heating scenario under  $T_{outdoor} = 13.04$  °C (I = 1.5A), with a shaded area indicating air temperatures.

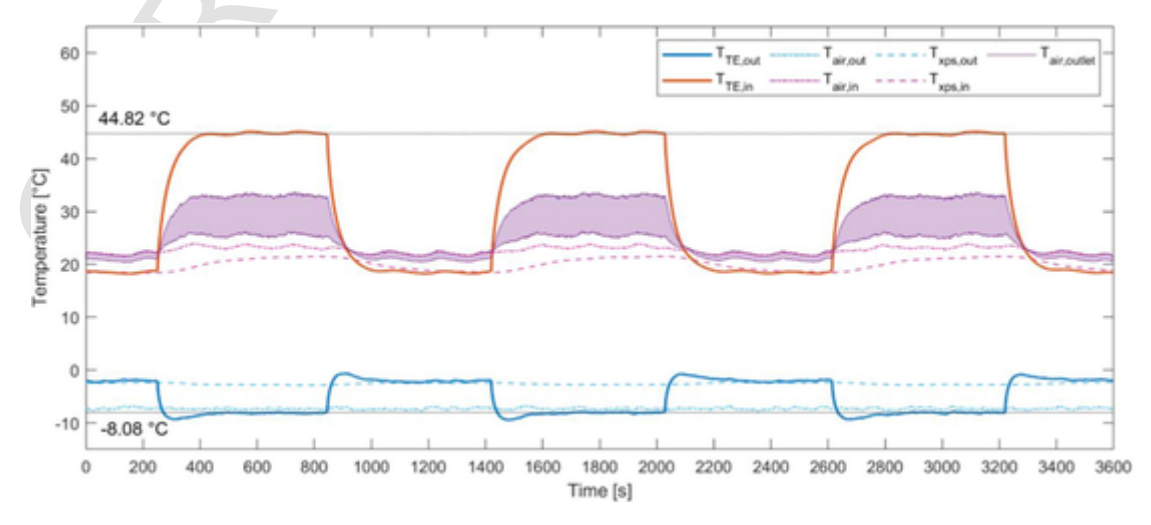


Fig. 6. Heating cycle performance of the TBE prototype in the coldest heating scenario with  $T_{outdoor} = -7.35$  °C,  $T_{indoor} = 23.34$  °C and current input of I = 1.5A.

temperature and air temperature changes are relatively stable (with a percentage change <1%) in three cycles.

#### 5.2. The impact of outdoor temperatures

The TBE prototype was tested under different outdoor temperatures (three for cooling and four for heating) to investigate the effect of outdoor conditions on TBE performance. The performance indicators selected include the surface temperatures of TEM, the thermal capacity of the TBE prototype, the effective thermal capacity of the prototype, and COP with and without fan power.

Fig. 7 shows the change trends of surface temperatures, COP, and both TEM and effective thermal capacity under outdoor conditions. As seen, a larger absolute temperature difference between indoor and outdoor air led to reductions in COP and thermal capacity. The cooling COP (with 1.5 A current input) was reduced from 0.51 to 0.38, along with an air temperature difference changed from 5.45 °C and 18.60 °C. An average reduction rate in cooling COP was 18% when the air temperature difference was greater than 10 °C. Conversely, the heating COP (with 1.5 A current input) was much higher and changed from 1.50 to 1.22, with an air temperature difference from about -5.78 °C and -30.69 °C. An average reduction rate in heating COP was 8% when the air temperature difference was greater than 10 °C. It shows that the heating COP of TBE is almost three times the cooling COP. The experimental data concludes that the heating performance of the TBE prototype is better than its cooling performance. Moreover, the heating COP of TBE performs better than that of an electric heater, a conventional device for heating with COP no larger than 1.0. Therefore, TBE is a promising alternative to traditional heating systems in buildings.

In addition, fan power consumption reduced the value of COP for both heating and cooling by around 6%–7%, as shown in Fig. 7. The performance of the envelope associated with the TBE prototype reduced COP by 12%–50% for cooling and 4%–31% for heating. This is because the TBE prototype used a thin layer of insulation. Hence, thicker XPS insulation with proper design to reduce heat loss and air leakage is recommended while ensuring the high-speed airflow around the heat sink for heat dissipation.

The thermal capacity is another key performance indicator, which determines the heat flux dissipated from TEMs. With a 1.5 A current input, the cooling, and heating capacity of the TBE prototype are approximately 8-9 W and 25-29 W, respectively. The effective thermal capacity, as mentioned in Eq. (3) in Section 4.2, which considers the heat loss through the whole TBE prototype, is a more appropriate indicator than thermal capacity for sizing TBE systems. Approximately 17 W of effective thermal capacity can be obtained as an active heating source for the indoor space in winter with an outdoor temperature of -7.35 °C. It is observed that the larger the absolute temperature difference between indoor and outdoor air, the larger the heat loss transferring across these construction materials can be observed. If a room needs a heating load of about 80 W to maintain a room temperature at 20 °C, the findings here indicate that five modular TBE prototypes (under 1.5 A current input) are needed. Additionally, test results reveal that TBE systems are more suitable for use in warm climate zones such as zone 3 and zone 4 [22]. However, the optimal design of TBE varies from region to region, so more design optimization studies are highly needed.

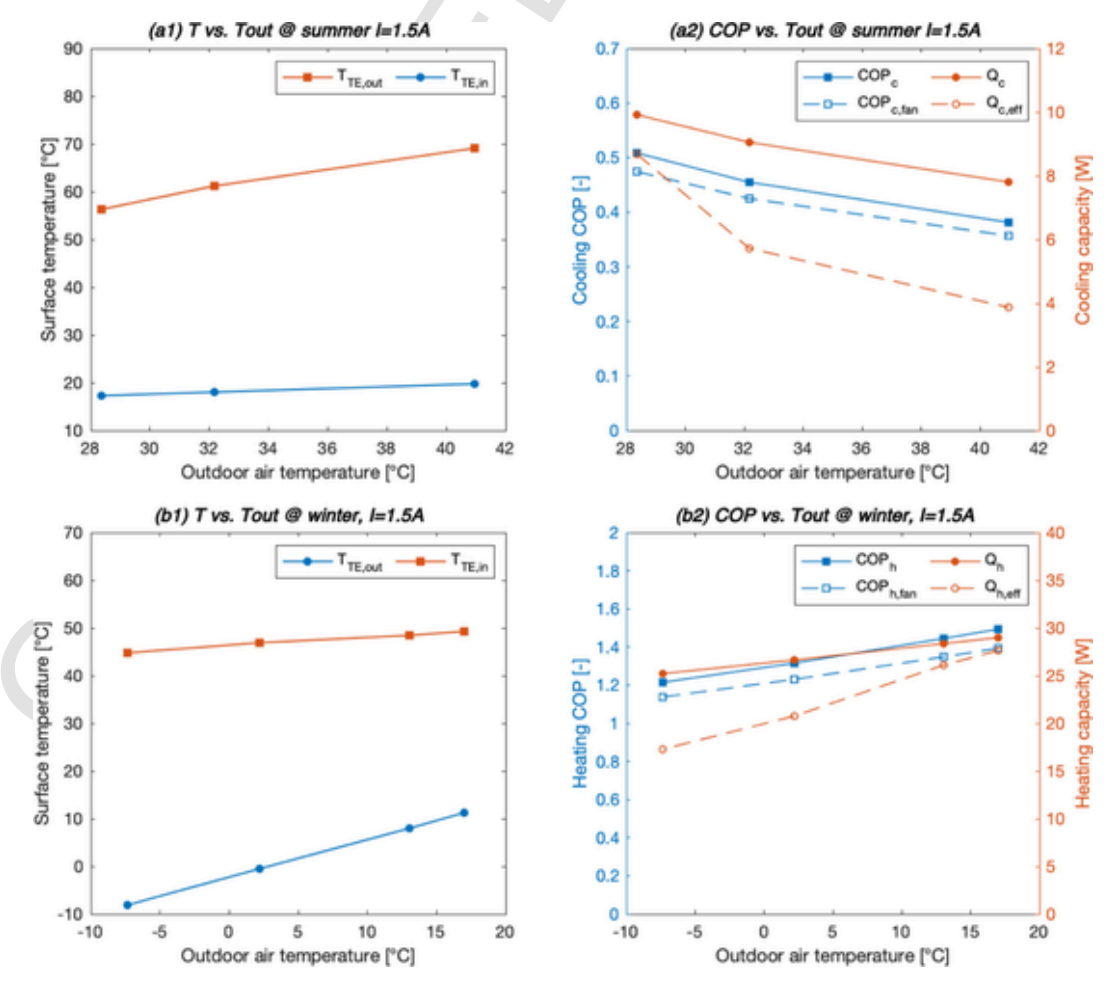


Fig. 7. Steady-state surface temperatures, COP, and capacity of TBE in (a) a cooling scenario in summer and (b) a heating scenario in winter.

## 5.3. The impact of the current input

The experimental data indicates that power input can significantly influence TBE performance. The TBE prototype performance was tested and analyzed under the same temperature conditions but with different current inputs ranging from 0.3 A to 1.5 A. An outdoor air temperature was set at 32.17  $^{\circ}\text{C}$  and 13.04  $^{\circ}\text{C}$  for the cooling and heating seasons, respectively, using the same performance indicators.

As seen in Fig. 8(a1, b1 and c1), the greater power input leads to a more significant difference between the surface temperatures of TEM. The temperature increase on the hot side is larger than the simultane-

ous temperature drop on the cold side. A similar phenomenon can be found in the thermal capacity, as shown in Fig. 8(a2, b2 and c2). The cooling capacity increases as the current increases, but the increase tends to converge. However, current and heating capacity are almost linear during the heating season. The result is further proof that TBE has better heating performance. But in the colder condition, larger power input is needed to provide effective heating. In Fig. 8(c2), the effective thermal capacity becomes negative with a current input of 0.5 A. This is because a large temperature difference between indoor and outdoor air leads to more heat loss across the TBE.

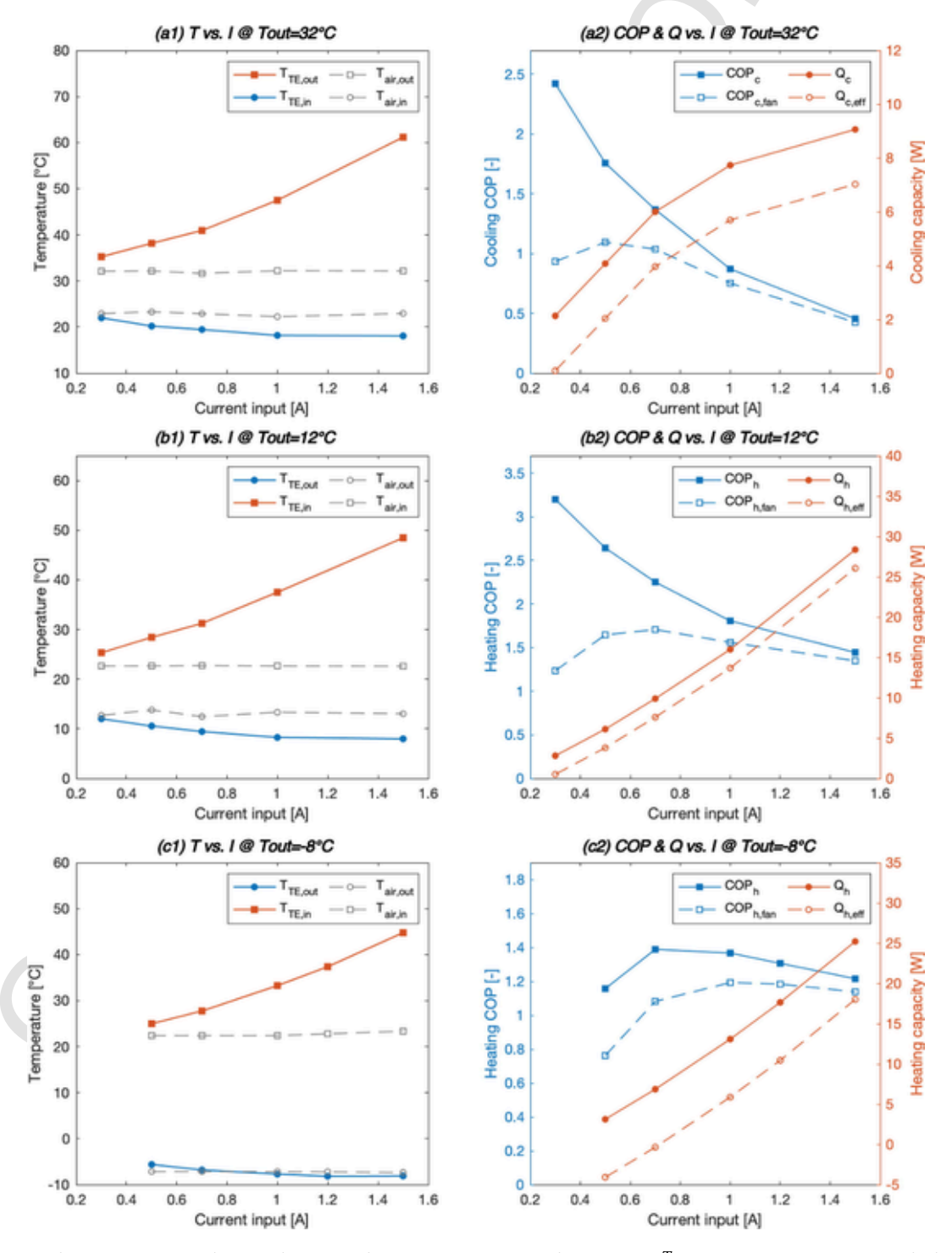


Fig. 8. Steady-state surface temperatures and COP and capacity of TBE in (a1-a2) warm cooling scenario ( $T_{outdoor}$  = 32.17 °C, I = 0.3–1.5A), (b1-b2) warm heating scenario ( $T_{outdoor}$  = 13.04 °C, I = 0.3–1.5A), and (c1-c2) coldest heating scenario ( $T_{outdoor}$  = -7.35 °C, I = 0.5–1.5A).

In addition, the COP also varies with the current input. COP decreases with the current increase from 0.3 A to 1.5 A in heating and cooling. The Joule heat and the heat conduction are larger than Peltier heat. Joule heat and heat conduction are considered heat losses in the cooling mode, decreasing cooling performance. Thus, TBE works better in the heating mode in winter since Joule heat, becoming heating gains, improves the heating capacity. After considering the power consumed by the fan, the COP curve shows a different trend. The COP, including fan power, increases and then decreases with a larger current. The maximum COP with fan power determines the optimal operating current, which is approximately 0.5 A to 0.7 A for the cooling and heating seasons. The highest cooling COP including fan power is 1.1, and the highest heating COP is 1.7. Different optimal current inputs (from 0.5 A to 1 A) in the coldest heating case yield the highest COP at 1.4 and COP considering fan power at 1.15. In this case, fan power consumption reduced the value of COP for both heating and cooling by around 7%-61% with improving current. The envelope's performance associated with the TBE prototype reduced COP by 22%-96% for cooling and 8%-81% for heating with increasing current.

The result gives a guide for the design, control, and operation of the TBE system. Given outdoor temperature in the design condition, the optimal current input can be determined in the process. According to the corresponding thermal capacity, the number of TEMs and area of TBE can be decided. For the TBE operation in a partial load, due to the flexibility of the TBE system, the controller can decide the numbers of TEMs to be operated according to the optimal power input and its thermal capacity.

## 5.4. The impact of fan

To study the impact of the fan status on the TBE performance, the prototype was tested in two different operating conditions, controlled by an interior fan attached to the heat sink of the TBE. The fan was turned on during the first test and off during the second test while remaining all other conditions the same. In the tests, outdoor air temperatures were 32.17  $^{\circ}$ C for cooling and 13.04  $^{\circ}$ C for heating. The current input was 0.7 A. Fig. 9 compares the COP and thermal capacity with the fan on and off.

Fig. 9(a) shows the temperatures of TBE surfaces in the cooling when the fan was turned on and off. In the test, the interior fan was turned off after the TBE system reached a steady state at around 400 s with a sudden change in surface temperature on the indoor side. In this case, the cold side of TEM could not transfer cooling power to the indoor air effectively, so the surface temperature dropped to a minimum of 9 °C, much lower than the indoor temperature. With one fan turned off, the TBE prototype took longer to reach another steady state (at around 20 min). The COP and capacity (Fig. 9(b)) obtained under this operating condition were lower than the case with two fans running. As a result, the COP decreased by 36%, and the cooling capacity decreased by 40%.

For the heating, as shown in Fig. 9(c), the interior fan was turned off after the TBE system reached a steady state. Similarly, the surface temperature on the indoor side changed dramatically, and the hot side of TEM could not release heat to the indoor air effectively. Hence, the surface temperature increased to 60 °C. The COP and capacity (Fig. 9(d)) were lower under operating conditions than with two fans running. As a result, the COP decreased by 43%, and the heating capacity decreased by 40%. It is found that, although the surface temperature changed dramatically without forced air convection, the thermal capacity also reduced significantly due to the insufficient heat transfer at the surface. Therefore, maintaining a higher heat transfer coefficient at the boundary is required for better TBE performances. Strong forced convection can lead to higher energy consumption, while radiant heating could be a better choice where heat is primarily dissipated by radiation.

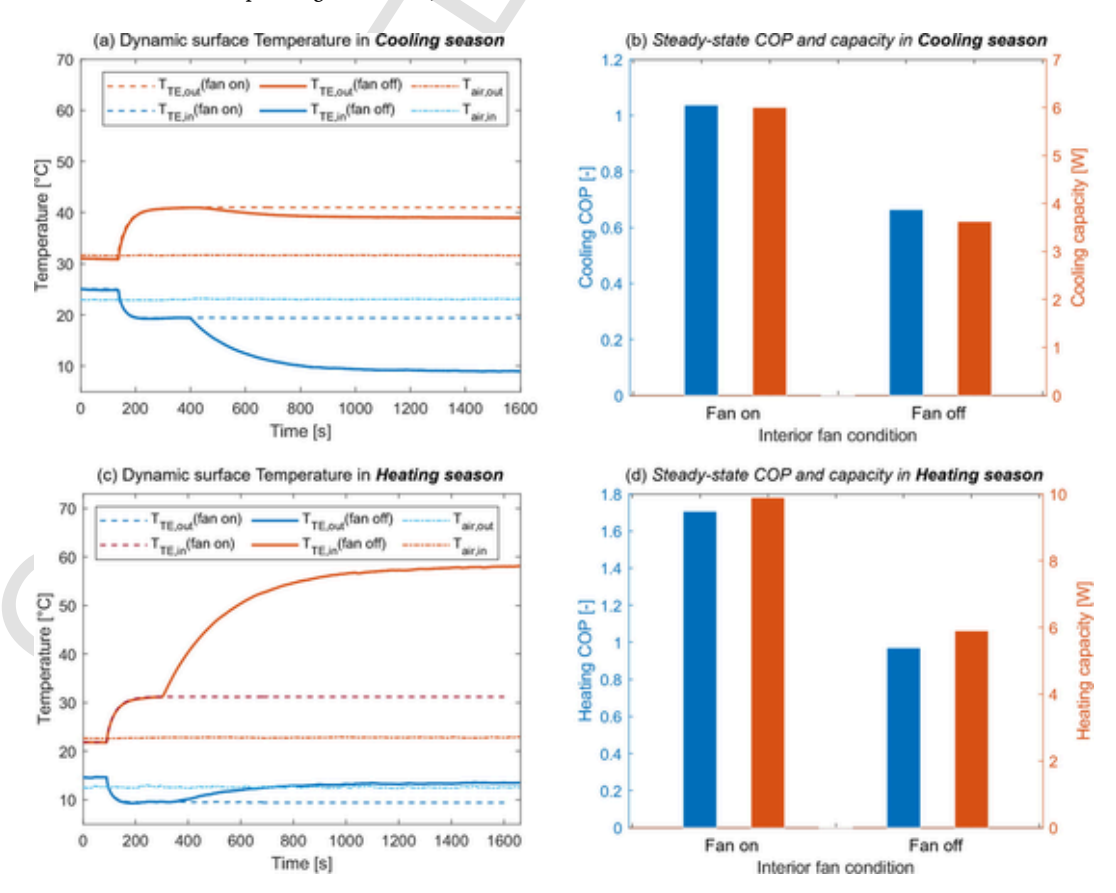


Fig. 9. (a) Temperature and (b) the comparison of COP and capacity of TBE prototype with fan control in a cooling season (I = 0.7A,  $T_{outdoor}$  = 32.17 °C), and (c) temperature, and (d) the comparison of COP and capacity with fan control in a heating season (I = 0.7A,  $T_{outdoor}$  = 13.04 °C).

#### 5.5. Summary

Table 4 summarizes the testing results discussed in *Section 5*. TBE has a maximum thermal capacity of 29 W for heating tests, a highest heat flux density of 190.4 W/m², and a maximum COP of 3.2. The largest heating COP considering fan power (1.7) obtained in the test is 1.7 times the efficiency of an electric heater (with a theoretical efficiency lower than 1 [23]). The tall heat sink in the studied TBE prototype helps dissipate heat effectively to the surroundings with its large surface area. The high-performance TEM also contributes to the efficiency (a figure of merit ZT of around 0.7 at 300 K). For cooling tests, TBE has a maximum thermal capacity of 9.9 W, a maximum heat flux density of 59.8 W/m², and a maximum COP of 2.4. The cooling COP of TBE is lower than typical vapor compression devices.

Moreover, the results show that TBE is always more effective in heating than cooling for the same absolute air temperature difference and current input. The electric power input is mainly consumed for generating Joule heat and active heat absorption and discharge (Peltier heat) on two sides of the TEM. Firstly, Joule heat counteracts part of the cooling effect and favors the heating effect. Secondly, considering the constant current and the Seebeck coefficient, the Peltier heat is linearly related to the surface temperature. This means the hot side has a more significant Peltier heat  $(SIT_h)$  to release, whereas the cold side has less Peltier heat  $(SIT_c)$  to absorb. Combining these two reasons, TBE operated in heating has better performance and higher COP (no consideration of fan power) than cooling.

The heat flux density depends on the current input and can achieve over 100 W per unit surface area of the TBE prototype, equivalent to the maximum one of a radiant floor system. The heat flux density is a critical parameter to determine the area of the TBE prototype with consideration of cost and thermal comfort. For example, a room requiring a heat load of 250 W needs at least  $2.5 \, \text{m}^2$  of the conventional building envelope to be replaced with TBE if the desired heat flux density is around  $100 \, \text{W/m}^2$ .

Operating temperature affects the performance and design of the TBE system. An average of 7.5% reduction in heating COP and 18% reduction in cooling COP was found with an absolute 10 °C greater temperature difference between indoor and outdoor air. The effective thermal capacity decreased more with more severe outdoor conditions. Therefore, TBE systems are more suitable for use in mild heating climate zones, such as ASHRAE zone 3 and 4. On the other hand, the optimal design of TBE varies from region to region, so more design optimization studies are needed for further studies.

The current input can control the surface temperature, thermal capacity, and heat flux density as desired. For a single prototype operating in warm heating and cooling cases with current input of 0.3–1.5 A, the highest COP is always obtained with a slight current input. How-

Table 4
Summary of testing results.

Function	T <sub>SA,out</sub> [°C]	T <sub>SA,in</sub> [°C]	I <sub>input</sub> [A]	Thermal capacity [W]	COP	Heat flux density [W/m²]
Cooling	28.36	22.35	1.5	9.9	0.5	59.8
	32.17	22.92	0.3–1.5	1.9–8.7	0.5– 2.4	0.6–48.6
	32.17	22.92	0.7 (Fan off)	3.6	0.7	24.0
	40.95	22.91	1.5	7.8	0.4	26.7
Heating	16.99	22.77	1.5	29.0	1.5	190.4
	13.04	22.61	0.3–1.5	2.8–28.4	1.5– 3.2	3.5–179.5
	13.04	22.61	0.7 (Fan off)	5.9	1.0	39.3
	2.20	23.58	1.5	28.4	1.32	1.8
	-7.35	23.34	0.5–1.5	3.1–25.2	1.2– 1.4	-28.1-124.0

ever, it is not valid for TBE in colder weather with an outdoor temperature of  $-7.35\,^{\circ}$ C. A minimum current of 0.7 A is needed to provide active heating to the space in this condition. Moreover, there has an optimal current input that leads to the maximum COP considering fan power. The highest COP considering fan power is 1.1 and 1.7 in cooling and heating modes, respectively. This result can guide the control and operation of TBE.

Boundary thermal resistance of TEM inside TBE is also an important parameter that affects the system performance. Boundary conditions usually involve radiation or forced convection. Test results indicate that COP and thermal capacity can reduce by about 40% with the interior fan turned off. However, the increase in energy consumption associated with lowering the boundary thermal resistance also needs to be considered. Therefore, energy-efficient heat dissipation becomes an important measure to improve TBE performance.

#### 6. Conclusion and future work

A TBE prototype for space heating and cooling was designed, constructed, and evaluated in a laboratory environment. The prototype was tested at an indoor temperature of 22.35-23.58 °C and outdoor temperatures from -7.35 °C and 16.99 °C for heating and from 28.36 °C to 40.95 °C for cooling, with varied power inputs and fan conditions. The TBE can be significantly affected by different operating conditions including outdoor air temperature, power input, boundary heat transfer, etc. Experimentally, the maximum COP of TBE in heating mode is 3.2. The average heating COP of TBE with a current of 1.5 A and the outdoor temperature of -7.35 - +16.99 °C is 1.37. The average heating COP of TBE operating with the current of 0.3–1.5 A at an outdoor temperature of 13.04 °C is 2.27. Based on the test result, TBE has a higher COP for heating, around three times the one for cooling. Moreover, the TBE system demonstrates a better heating efficiency than an auxiliary electric heater (efficiency at 1.0) for the heat pump system. Therefore, the TBE system can be a promising alternative to a conventional heating system

The following recommendations are made for future work:

- High-performance thermoelectric material. Developing thermoelectric materials with a higher ZT at ambient conditions is essential for enhancing the overall system performance and system integrity [24,25]. In building applications, lower thermal conductivity is desirable and could be achieved by developing thermoelectric composite materials, foam-structured materials, doped cementitious materials, etc.
- 2. Energy-efficient heat dissipation technology. The enhancement of boundary heat transfer with energy-efficient technology is another approach to achieving higher heat pumping performance. Since radiant heating can eliminate the use of a circulation fan and its associated energy consumption, the radiant TBE system needs to be studied. The integration of energy recovery ventilation with TBE system design could be a further step towards improving efficiency.
- 3. Optimal design and control. The current TEM in the market is designed for electronic cooling and thus does not have the optimal design for building applications. A more holistic study on the optimal TEM design for TBE use is necessary. The TBE performance is significantly impacted by a variety of operating conditions, requiring a smart and predictive control strategy to be applied in a real-world environment for reliable performance.
- 4. Whole building simulation. Simulating TBE-integrated buildings is vital to determining their long-term performance and their economic and environmental benefits. A future research topic could be the whole building simulation under dynamic controls and outdoor conditions.

## CRediT authorship contribution statement

Xiaoli Liu: Methodology, Investigation, Writing – original draft. Kazuaki Yazawa: Supervision, Writing – review & editing. Ming Qu: Conceptualization, Supervision, Writing – review & editing. Orkan Kurtulus: Resources. Brian Norton: Writing – review & editing. Niall Holmes: Writing – review & editing. Ruchita Jani: Writing – review & editing. Jorge Kohanoff: Writing – review & editing. Lorenzo Stella: Writing – review & editing. Conrad Johnston: Writing – review & editing. Hongxi Yin: Writing – review & editing.

#### **Declaration of Competing Interest**

The authors declare the following financial interests/personal relationships which may be considered as potential competing interests: Ming Qu reports financial support was provided by National Science Foundation.

## Data availability

Data will be made available on request.

## Acknowledgment

This material is based upon work supported by the National Science Foundation under Grant No. CBET-1805818.

#### References

- [1] U.S. Energy Information Administration. Annual Energy Outlook 2021 n.d. <a href="https://www.eia.gov/outlooks/aeo/">https://www.eia.gov/outlooks/aeo/</a> (accessed April 22, 2021).
- [2] D.M. Rowe, Thermoelectrics handbook: macro to nano, Thermoelectrics Handbook Macro to Nano. 80 (2005) 1014, https://doi.org/10.1038/ki.2011.318.
- [3] K. Irshad, K. Habib, R. Saidur, M.W. Kareem, B.B. Saha, Study of thermoelectric and photovoltaic facade system for energy efficient building development: A review, Journal of Cleaner Production. 209 (2019) 1376–1395, https://doi.org/ 10.1016/j.jclepro.2018.09.245.
- [4] A. Zuazua-Ros, C. Martín-Gómez, E. Ibañez-Puy, M. Vidaurre-Arbizu, Y. Gelbstein, Investigation of the thermoelectric potential for heating, cooling and ventilation in buildings: Characterization options and applications, Renewable Energy. 131 (2019) 229–239, https://doi.org/10.1016/j.renene.2018.07.027.
- [5] S.Y. Cheon, H. Lim, J.W. Jeong, Applicability of thermoelectric heat pump in a dedicated outdoor air system, Energy. 173 (2019) 244–262, https://doi.org/ 10.1016/j.energy.2019.02.012.
- [6] Y. Luo, L. Zhang, Z. Liu, J. Yu, X. Xu, X. Su, Towards net zero energy building: The application potential and adaptability of photovoltaic-thermoelectric-battery wall system, Applied Energy. 258 (2020), https://doi.org/10.1016/ j.apenergy.2019.114066.
- [7] Finn PA, Asker C, Wan K, Bilotti E, Fenwick O, Nielsen CB. Thermoelectric Materials: Current Status and Future Challenges. Frontiers in Electronic Materials 2021;0:1. <a href="http://doi.org/10.3389/femat.2021.677845">http://doi.org/10.3389/femat.2021.677845</a>>.
- [8] Z. Liu, L. Zhang, G. Gong, H. Li, G. Tang, Review of solar thermoelectric cooling technologies for use in zero energy buildings, Energy and Buildings. 102 (2015) 207–216, https://doi.org/10.1016/j.enbuild.2015.05.029.
- [9] D.S. Godwin, R. Ferenchiak, The implications of residential air conditioning

- refrigerant choice on future hydrofluorocarbon consumption in the United States, Journal of Integrative Environmental Sciences. 17 (2019) 29, https://doi.org/10.1080/1943815x.2020.1768551.
- [10] W. Zhu, Y. Deng, Y. Wang, A. Wang, Finite element analysis of miniature thermoelectric coolers with high cooling performance and short response time, Microelectronics Journal. 44 (2013) 860–868, https://doi.org/10.1016/ j.mejo.2013.06.013.
- [11] R.A. Khire, A. Messac, S. Van Dessel, Design of thermoelectric heat pump unit for active building envelope systems, International Journal of Heat and Mass Transfer. 48 (2005) 4028–4040, https://doi.org/10.1016/j.ijheatmasstransfer.2005.04.028.
- [12] Z. Liu, L. Zhang, G. Gong, T. Han, Experimental evaluation of an active solar thermoelectric radiant wall system, Energy Conversion and Management. 94 (2015) 253–260, https://doi.org/10.1016/j.enconman.2015.01.077.
- [13] Z. Liu, L. Zhang, G. Gong, Y. Luo, F. Meng, Evaluation of a prototype active solar thermoelectric radiant wall system in winter conditions, Applied Thermal Engineering. 89 (2015) 36–43, https://doi.org/10.1016/ j.applthermaleng.2015.05.076.
- [14] C. Wang, C. Calderón, Y. Wang, An experimental study of a thermoelectric heat exchange module for domestic space heating, Energy and Building.s 145 (2017) 1–21, https://doi.org/10.1016/j.enbuild.2017.03.050.
- [15] C. Martín-Gómez, A. Zuazua-Ros, Del Valle, K. de Lersundi, B. Sánchez Saiz-Ezquerra, M. Ibáñez-Puy, Integration development of a Ventilated Active Thermoelectric Envelope (VATE): Constructive optimization and thermal performance, Energy and Buildings. 231 (2021), https://doi.org/10.1016/ienbuild.2020.110593.
- [16] A. Zuazua-Ros, C. Martín-Gómez, E. Ibáñez-Puy, M. Vidaurre-Arbizu, M. Ibáñez-Puy, Design, assembly and energy performance of a ventilated active thermoelectric envelope module for heating, Energy and Buildings. 176 (2018) 371–379. https://doi.org/10.1016/j.enbuild.2018.07.062.
- [17] E. Ibáñez-Puy, C. Martín-Gómez, J. Bermejo-Busto, A. Zuazua-Ros, Thermal and energy performance assessment of a thermoelectric heat pump integrated in an adiabatic box, Applied Energy. 228 (2018) 681–688, https://doi.org/10.1016/ iapenergy.2018.06.097.
- [18] M. Ibañez-Puy, J. Bermejo-Busto, C. Martín-Gómez, M. Vidaurre-Arbizu, J.A. Sacristán-Fernández, Thermoelectric cooling heating unit performance under real conditions, Applied Energy. 200 (2017) 303–314, https://doi.org/10.1016/j.apenergy.2017.05.020.
- [19] C. Martín-Gómez, M. Ibáñez-Puy, J. Bermejo-Busto, J.A. Sacristán Fernández, J.C. Ramos, A. Rivas, Thermoelectric cooling heating unit prototype, Building Services Engineering Research and Technology. 37 (2016) 431–449, https://doi.org/10.1177/0143624415615533.
- [20] Fraisse G, Ramousse J, Sgorlon D, Goupil C. Comparison of different modeling approaches for thermoelectric elements. Energy Conversion and Management 2013;65:351–6. <a href="http://doi.org/10.1016/j.enconman.2012.08.022">http://doi.org/10.1016/j.enconman.2012.08.022</a>.
- [21] Fornasini P. The Uncertainty in Physical Measurements. The Uncertainty in Physical Measurements 2008. <a href="http://doi.org/10.1007/978-0-387-78650-6">http://doi.org/10.1007/978-0-387-78650-6</a>.
- [22] Baechler MC, Gilbride TL, Cole PC, Hefty MG, Ruiz K. Guide to Determining Climate Regions by County PREPARED BY Pacific Northwest National Laboratory 2015.
- [23] Electric Resistance Heating | Department of Energy n.d. <a href="https://www.energy.gov/energysaver/electric-resistance-heating">https://www.energy.gov/energysaver/electric-resistance-heating</a> (accessed January 1, 2022).
- [24] Ibáñez M, Luo Z, Genç A, Piveteau L, Ortega S, Cadavid D, et al. High-performance thermoelectric nanocomposites from nanocrystal building blocks. Nature Communications 2016 7:1 2016;7:1–7. <a href="http://doi.org/10.1038/ncomms10766">http://doi.org/10.1038/ncomms10766</a>.
- [25] Liu X, Jani R, Orisakwe E, Johnston C, Chudzinski P, Qu M, et al. State of the art in composition, fabrication, characterization, and modeling methods of cementbased thermoelectric materials for low-temperature applications. Renewable and Sustainable Energy Reviews n.d.;137:110361. < http://doi.org/10.1016/ j.rser.2020.110361 >.